RESEARCH ARTICLE

Purification of mitochondria from skeletal muscle tissue for transcriptomic analyses reveals localisation of nuclear-encoded non-coding RNAs

Authors:

Jessica Silver[1] and Adam J. Trewin[1,6] (co-first authors), Stella Loke[2], Larry Croft[2], Mark Ziemann[3,7], Megan Soria[3], Hayley Dillon[1,4], Søren Nielsen[5], Séverine Lamon[1], Glenn. D. Wadley[1]

Affiliations:

[1]Institute for Physical Activity and Nutrition, School of Exercise and Nutrition Sciences, Deakin University, Geelong, Victoria, Australia.

[2]Genomics Centre, School of Life and Environmental Sciences, Deakin University, Geelong, Victoria, Australia.

[3]School of Life and Environmental Sciences, Deakin University, Geelong, Victoria, Australia.

[4]Human Integrated Physiology and Sports Cardiology Laboratory, Baker Heart and Diabetes Institute, Melbourne, Australia.

[5]The Centre of Inflammation and Metabolism and the Centre for Physical Activity Research, Rigshospitalet, University of Copenhagen, Copenhagen, Denmark.

[6]Department of Anatomy and Physiology, University of Melbourne, Australia.

[7]Burnet Institute, Melbourne, Australia

Corresponding author:

Prof. Glenn Wadley

Deakin University

Institute for Physical Activity and Nutrition,

School of Exercise and Nutrition Sciences,

Australia

3125

Email: glenn.wadley@deakin.edu.au

ABSTRACT

Mitochondria are central to cellular function, particularly in metabolically active tissues such as skeletal muscle. Nuclear-encoded RNAs typically localise within the nucleus and cytosol but a small population may also translocate to subcellular compartments such as mitochondria. We aimed to investigate the nuclear-encoded RNAs that localise within the mitochondria of skeletal muscle cells and tissue. Intact mitochondria were isolated via immunoprecipitation (IP) followed by enzymatic treatments (RNase-A and proteinase-K) optimised to remove transcripts located exterior to mitochondria, making it amenable for high-throughput transcriptomic sequencing. Small-RNA sequencing libraries were successfully constructed from as little as 1.8 ng mitochondrial RNA input. Small-RNA sequencing of mitochondria from rat myoblasts revealed the enrichment of over 200 miRNAs. Whole-transcriptome RNA sequencing of enzymatically-purified mitochondria isolated by IP from skeletal muscle tissue showed a striking similarity in the degree of purity compared to mitoplast preparations which lack an outer mitochondrial membrane. In summary, we describe a novel, powerful sequencing approach applicable to animal and human tissues and cells that can facilitate the discovery of nuclear-encoded RNA transcripts localised within skeletal muscle mitochondria.

48 **INTRODUCTION**

49 Mitochondria are subcellular organelles essential for numerous cellular processes including energy
50 metabolism, signalling, ion and redox homeostasis as well as regulation of apoptosis (Spinelli and
51 Haigis, 2018). Mitochondria are comprised of proteins encoded by both the nuclear and mitochondrial
52 genomes, but nuclear-encoded RNAs are not usually localised within mitochondria. A small number of
53 specific nuclear-encoded non-coding RNAs (ncRNAs), such as microRNAs (miRNAs) (Barrey et al.,
54 2011, Sripada et al., 2012, Das et al., 2012) and possibly long non-coding RNAs (lncRNAs) (Noh et
55 al., 2016) can however be imported into mitochondria (Silver et al., 2018). This may occur via the
56 polynucleotide phosphorylase (Wang et al., 2010) and other putative transport mechanisms (reviewed
57 in Silver et al., 2018). Because ncRNAs have the ability to regulate various transcriptional and
58 translational processes relating to mitochondrial function, it is of interest to determine which of these
59 may localise within mitochondria in order to understand the nature of their potential regulatory actions.

60 Investigations into mitochondria-localised nuclear-encoded RNAs have been constrained, first, by the
61 technical challenges of obtaining pure mitochondrial preparations free of confounding RNAs peripheral
62 to isolated mitochondria and, second, by the significantly lower RNA yields from subcellular fractions
63 when compared to whole tissue homogenates. Early studies providing evidence for the localisation of
64 ncRNAs within mitochondria stem from micro-array analysis and were routinely validated by single
65 qPCR assays or *in situ* hybridisation (Barrey et al., 2011, Sripada et al., 2012, Das et al., 2012).
66 However, the overall population of ncRNAs that localise within mitochondria and their regulatory
67 actions, particularly within metabolically active tissues remains largely unknown.

68 Skeletal muscle constitutes ~40% of human body mass and plays a central role in whole body
69 metabolism (Zurlo et al., 1990). To meet these dynamic bioenergetic demands, skeletal muscle is
70 densely populated with mitochondria (Russell et al., 2014). Thus, gaining a greater understanding of
71 the RNA profile within muscle mitochondria may yield important insights into the cellular biology and
72 aetiology of diverse metabolic diseases characterised by mitochondrial dysfunction, such as diabetes
73 mellitus and chronic myopathies (Silver et al., 2018). Here, we report a method for isolating and
74 optimising the enzymatic purification of mitochondria from rodent muscle cells or tissues. We provide
75 direct evidence for the purity of this mitochondrial fraction, making it amenable for downstream high-
76 throughput analyses. We also describe methods for small-RNA and whole transcriptome sequencing of
77 mitochondria isolated from cultured myoblasts as well as skeletal muscle tissue samples from animals
78 and humans.

RESULTS

Protease purification of isolated mitochondria from myoblasts

We first isolated mitochondria from cultured L6 rat myoblasts using an antibody against an outer mitochondrial membrane protein (TOMM22) conjugated to magnetic beads allowing for precipitation of intact isolated mitochondria (Figure 1). Immunoblot of the post-precipitation mitochondrial fraction revealed that a small amount of α-tubulin and Lamin B1 (used as protein markers of the cytosol and nucleus, respectively) were present in the isolated mitochondria fraction (Figure 2, lane 1). A portion of the isolated mitochondria was incubated with the serine protease, proteinase-K, to digest proteins not located within the mitochondrial intermembrane space (IMS) or matrix compartments. This led to depletion of α-tubulin and Lamin B1, in addition to a marker of the outer mitochondrial membrane (TOMM20), while intermembrane space (cytochrome-*c*) and matrix protein markers (citrate synthase) were protected from digestion (Figure 2, lane 2). All proteins probed were susceptible to proteinase-K when mitochondrial membranes were dissolved in the presence of the detergent triton-X (Figure 2, lane 3). Together, this demonstrates that mitochondrial isolation by TOMM22-immunoprecipitation followed by enzymatic treatment yields a purified, intact mitochondrial fraction suitable for downstream protein analyses. Based on this, we hypothesised that an analogous approach utilising a ribonuclease could be used to remove RNA located outside of isolated mitochondria.

Ribonuclease purification of isolated mitochondria from myoblasts

Next, mitochondria isolated from L6 rat myoblasts were exposed to a range of concentrations of RNase-A, an endonuclease that cleaves phosphodiester bonds after pyrimidine residues in the RNA molecule (Witzel, 1963). RNase-A-treated isolated mitochondria were assessed by RT-qPCR for abundance of mtDNA-encoded mRNA (*Mt-co3*) localised exclusively within the mitochondrial matrix compartment, and a nuclear-encoded mRNA (*Cox4i1*) that localises outside mitochondria (Suissa and Schatz, 1982). We found that *Mt-co3* was protected from degradation at RNase concentrations up to at least 100 µg/mL, whereas partial *Cox4i1* degradation occurred at 10 µg/mL and was mostly degraded at 100 µg/mL (Figure 3). In the presence of detergent to disrupt mitochondrial membranes, 1 µg/mL RNase-A was sufficient to digest all *Cox4i1* and *Mt-co3*, as well as an exogenous mRNA spike-in control (Figure 3). This suggests that a certain proportion of cytosolic *Cox4i1* is protected from digestion at lower RNase-A concentrations, potentially as a result of being bound to ribosomes at the outer mitochondrial membrane (Gold et al., 2017). Taken together, these data suggest that TOMM22-IP mitochondrial isolation followed by RNase-A treatment is suitable for downstream mitochondrial RNA analyses provided the RNase-A concentration is sufficient to remove transcripts not located within the mitochondrial membranes.

113 Small RNA sequencing on purified isolated mitochondria from myoblasts reveals mitochondria
114 localised miRNAs

115 We next aimed to optimize a protocol to perform transcriptomic analysis of the small RNAs (sRNA)
116 contained within isolated mitochondria from L6 rat myoblasts. We first prepared sRNA libraries from
117 120 ng and 60 ng mitochondrial RNA with 0.5X adapter dilutions (NEBNext 3′ and 5' SR Adaptors,
118 and RT primer for Ilumina), in line with the standard manufacturer protocol (NEBNext Multiplex Small
119 RNA Library Prep Set (New England Biolabs). The standard protocol produced large amounts of
120 adapter-dimer and was not sufficient to ligate adapters to the target miRNAs within the sample
121 (Supplementary Figure 1 A, B). We next decreased the amount of the 3' and 5' adapters to investigate
122 if a lower molar ratio improved miRNA ligation efficiency. Both the modified-0.3X (Supplementary
123 Figure 1C) and modified-0.1X (data not shown) approaches produced quantifiable amounts of the target
124 miRNA library when prepared from 60 ng mitochondrial RNA, although the total cDNA yield was
125 approximately 7-fold higher from the modified-0.3X when compared to modified-0.1X protocol. Both
126 modified approaches did decrease, but not prevent, adapter-dimer formation.

127 While 60 ng mitochondrial RNA is below the recommended library RNA input (>100 ng, NEBiolabs,
128 Inc.), mitochondrial RNA yield from cell and tissue samples is often considerably below this threshold.
129 Thus, it was necessary to investigate if the modified-0.3X and modified-0.1X approach could similarly
130 produce the target miRNA library when prepared from much lower amounts of mitochondrial RNA.
131 The modified-0.3X (Supplementary Figure 1 C, D) and modified-0.1X (data not shown) approaches
132 both produced the target library when prepared from >1.8 ng (range 1.8-60 ng) mitochondria RNA.
133 Total cDNA yields were, on average, 4.3-fold higher ($p<0.05$) when using the modified-0.3X protocol
134 compared to the modified-0.1X. The presence of adapter-dimer dominated each library, regardless of
135 the mitochondrial RNA input amount used. To combat this, all uniquely indexed libraries were
136 combined in an equimolar pool and run across two lanes of a TBE polyacrylamide gel. The gel fragment
137 corresponding to the miRNA region was manually excised, extracted from the gel and then sequenced.
138 There were no differences in total RNA-seq reads ($p=0.79$) and total mapped miRNA reads ($p=0.19$)
139 between the modified-0.3X and modified-0.1X protocols (Figure 4A). Over 200 miRNAs were detected
140 across all but the lowest (1.8 ng, modified-0.1X) mitochondrial RNA inputs (Figure 4B). The number
141 of miRNAs detected appeared to plateau when libraries were prepared from 15-60 ng mitochondrial
142 RNA (Figure 4B) and suggests that RNA inputs of at least 15 ng are sufficient to detect most miRNAs
143 within a sample. Ultimately, either modified approach is suitable for the construction of miRNA
144 libraries. However, the significantly higher library yields make the modified-0.3X approach amenable
145 to library pooling, gel excision, and subsequent sequencing.

146 We next investigated the relative abundance of miRNAs sequenced from serial dilutions of
147 mitochondrial RNA input (1.8-30 ng), when compared to the highest mitochondria RNA input (60 ng).

148 Most miRNAs detected were common between libraries prepared from 60 ng mitochondria RNA and
149 the lower mitochondria RNA inputs (Figure 4C-E). Further to this, the relative abundance of miRNAs
150 was comparable between libraries prepared from the two highest RNA inputs (60 vs 30 ng; Figure 4E).
151 A small number of miRNA species were over- (8 miRNAs) and under-represented (5 miRNAs) within
152 libraries prepared from the highest RNA input (60 ng) when compared to lowest RNA input (1.8 ng;
153 Figure 4C). MiRNAs detected in the highest, but not lowest, RNA input displayed low expression levels
154 within the 60 ng sample, and together constituted a small proportion (1069 rpm) of total reads.
155 Interestingly, the skeletal muscle-enriched miR-1, miR-133a, miR-133b and miR-16 and miR-486,
156 predicted to have roles in the regulation of mitochondrial function (Nielsen et al., 2010, Russell et al.,
157 2013), were detected at higher mitochondria RNA inputs (60 and 30 ng), but not lower inputs (1.8-15
158 ng; Figure 4). In contrast, the let-7 family as well as the skeletal muscle-enriched miR-206 were highly
159 abundant in all samples, and together constituted 63±8% of all mapped miRNA reads. Importantly, the
160 relative distribution of miRNAs within each sample provides adequate representation across serial
161 dilutions of mitochondrial RNA, making it possible to accurately investigate differential miRNA
162 expression across unique cell and tissue samples with variable mitochondrial RNA yields.

163 Together, these data suggest that careful optimization is required when preparing sRNA libraries from
164 low amounts of RNA from purified mitochondria. To minimize adapter-dimer presence in sRNA
165 libraries, gel excision and purification of the target miRNA fraction is recommended. Importantly, our
166 data demonstrate that RNA-seq results were comparable across serial dilutions of mitochondrial RNA
167 input, suggesting that low mitochondria RNA input does not limit the number nor the relative
168 distribution of miRNA species that can be detected.

169 <u>The transcriptomic profile of enzymatically treated isolated mitochondria from rat skeletal muscle tissue</u>
170 <u>reveals a similar degree of purity as mitoplasts.</u>

171 Next, we applied the purification strategies described thus far to study the transcriptome of
172 mitochondria isolated from muscle tissue samples. From a pooled homogenate of rat skeletal muscle
173 tissue, we compared mitochondria isolated with our IP+enzymatic treatment method against
174 mitochondria isolated using a traditional differential centrifugation method. At the protein level,
175 mitochondria isolated by immunoprecipitation had no detectable ribosomal marker proteins and very
176 little abundance of peroxisome, golgi apparatus or endoplasmic reticulum marker proteins, which
177 contrasted with mitochondria obtained via the differential centrifugation method (Supplementary
178 Figure 2A&B). Next, to confirm the lack of co-purifying contaminants on the outer mitochondrial
179 membrane, we compared our IP isolated+enzymatic treated mitochondria with mitoplasts (i.e.
180 mitochondria whose OMM is removed or disrupted but with an IMM and matrix that remains intact).
181 We generated mitoplasts and confirmed that they were devoid of outer mitochondrial membrane
182 (OMM) proteins such as TOMM20 and inner mitochondrial membrane (IMM) and inter membrane

183 space (IMS) proteins such as mitofilin and AIF without the loss of mitochondrial matrix proteins such
184 as citrate synthase (Supplementary Figure 2C).

185 We then performed RNA-sequencing on four different mitochondrial sample types: *i*) RNase-A treated
186 mitoplasts, *ii*) RNase-A treated IP isolated mitochondria with or *iii*) without proteinase-K enzymatic
187 purification (to evaluate RNAs that may be bound to ribosomes on the OMM or other RNA binding
188 proteins which protect them from RNase-A), and *iv*) RNase-A treated mitochondria isolated via
189 differential centrifugation ("CrudeMito"). Principal component analysis of the transcriptomes of these
190 mitochondrial sample types revealed a separation along the first principal component between crude
191 mitochondria extracts isolated by differential centrifugation ("CrudeMito") compared with
192 mitochondria isolated via IP and treated with RNase-A and with or without proteinase-K treatment
193 (MitoRNase+ProtK and MitoRNase, respectively) or mitoplasts treated with RNase-A
194 ("MitoplastRNase") (Figure 5A). The overlap of the latter three suggests a high overall degree of
195 similarity of the transcriptomic profile between immunoprecipitation-based methods when compared
196 to the crude mitochondrial fraction. For this reason, the crude mitochondrial fraction was excluded from
197 further analysis.

198 There were no differentially expressed mtDNA-encoded genes (Figure 5B left panel) or nDNA-encoded
199 genes between MitoplastRNase and MitoRNase+ProtK (Figure 5C left panel). In contrast, there were
200 several DE genes (both mtDNA- and nDNA-encoded) between MitoRNase without proK and
201 MitoplastRNase (Figure 5B & 5C middle panel), and also between MitoRNase without proK and
202 MitoRNase+ProtK (Figure 5B & 5C right panel). The same pattern was observed for mtDNA- and
203 nDNA-encoded rRNAs and mitochondrial tRNAs (data not shown). Collectively, these data
204 demonstrate that mitochondria isolated via our method of immunoprecipitation followed by RNase-A
205 and proteinase-K treatments yield a transcriptome of similar purity to that of mitoplasts.

206 Next, we extracted RNA from IP+purified (RNase + ProtK) mitochondria and RNA from the
207 corresponding whole tissue from the gastrocnemius skeletal muscle of 9-week old rats (Supplementary
208 Figure 3A & B). Whole-transcriptome RNA sequencing (Supplementary Figure 3C - E) revealed that
209 the transcriptomes of these mitochondria had a high degree of purity as indicated firstly by a low relative
210 proportion of nuclear-encoded mRNAs unrelated to mitochondria, such as genes associated with muscle
211 sarcomere function i.e. myosin light (e.g. *Myl1*) and heavy (e.g. *Myh4* and *Myh7*) isoforms, α-actin
212 (*Acta1*) and troponins (e.g. *Tnnc2*, *Tnnt3*; Figure 6A). Secondly, the mitochondrial fraction also
213 contained a low relative abundance of nuclear-encoded OXPHOS genes (including *Cox4i1)*, as
214 expected (Figure 6B). Thirdly, there was similar abundance of all mtDNA-encoded OXPHOS mRNA
215 transcripts including *Mt-co3* between the whole tissue and mitochondrial fractions (Figure 6C). This
216 serves as an important internal control as mtDNA transcripts are expected to be present in both isolated
217 mitochondria and whole tissue in similar proportions.

218 Lastly, we confirmed the suitability of this approach with human muscle tissue biopsy samples. We
219 isolated and purified mitochondria from these samples and performed analysis via RT-qPCR. This
220 revealed the absence of *COX4I1,* used as marker of nuclear-encoded mRNA contamination, yet, several
221 muscle-enriched miRNAs including miR-206 were detected (Supplementary Table 1), which is
222 consistent with our results in L6 myoblasts.

223

224 **DISCUSSION**

225 Studies of subcellular fractions using high-throughput analyses requires careful consideration of
226 purification strategies to avoid confounding effects of contaminants. Here we report an optimised
227 method for purification of isolated mitochondria for downstream transcriptomic analysis. Revealing the
228 utility of this approach, we confirmed that miRNAs can be reliably detected in the mitochondria of L6
229 myoblasts even when libraries are prepared from RNA inputs well below the thresholds often
230 recommended by manufacturers.

231 Incubation of isolated mitochondria with RNase-A digests any contaminating extra-mitochondrial RNA
232 to ensure that only RNA species contained within the mitochondria membranes are identified in
233 downstream analyses. This is important when investigating transcripts that do not localise in one
234 subcellular compartment, but instead may be actively transported between compartments in response
235 to various physiological stimuli. RNase-A protocols differ substantially between studies that have
236 investigated mitochondrial RNA expression. In previous studies, RNase-A has been used at variable
237 final concentrations (5-50 µg/mL) (Barrey et al., 2011, Mercer et al., 2011, Zhang et al., 2014, Bandiera
238 et al., 2011) or has been omitted entirely (Das et al., 2012, Dasgupta et al., 2015, Lung et al., 2006,
239 Sripada et al., 2012). Here, we demonstrate that RNase-A concentrations of at least 100 µg/mL are
240 required to digest the majority of nuclear-encoded transcripts (such as *Cox4i1*) in rat myoblasts.
241 Importantly, this approach is transferable between cell and tissue models and is shown to effectively
242 degrade potentially contaminating, non-mitochondrial RNA in mitochondria isolated from human
243 skeletal muscle tissue (Supplementary Table 1).

244 Investigations into the mitochondrial RNA population are often limited by technical challenges. For
245 example, the inherently low mitochondrial RNA yields compared to total cellular RNA are well below
246 the threshold required for commercially available small RNA library preparation protocols. This
247 challenge may be overcome by combining mitochondria RNA from biological samples into pools that
248 represent a single 'intervention' or 'clinical' group, and the 'control' group (Jagannathan et al., 2015,
249 Wang et al., 2017). While this effectively increases the amount of mitochondrial RNA available for
250 sRNA library preparation, this approach introduces further limitations. First, the use of pooled samples
251 requires a much larger sample size to achieve the same statistical power (Takele Assefa et al., 2020).
252 Second, gene expression is highly variable between individuals; taking a pooled sample approach may

253 mask potential individual variability in miRNA expression (Takele Assefa et al., 2020, Rajkumar et al.,
254 2015). Our findings illustrate that small RNA libraries can be prepared from individual biological
255 samples without the need to pool multiple samples, thereby increasing the statistical power available,
256 especially for human studies with limited sample material and high participant burden.

257 A modified small RNA library preparation protocol increased ligation efficiency of the 3' and 5'
258 adapters to miRNAs within mitochondrial samples. However, this modified approach was not able to
259 prevent adapter-dimer formation entirely. As the adapter-dimer product is approximately 20 bp smaller
260 than adapter-ligated miRNAs and preferentially binds to the flow cell during RNA-Seq, gel extraction
261 of the target miRNA region is essential to maximise read counts that map to miRNAs rather than
262 adapter-dimer (Shore et al., 2016). When used together, the modified-0.3X protocol plus gel extraction
263 were successful in detecting over 200 miRNAs from L6 mitochondria RNA inputs as low as 1.8 ng.
264 Importantly, the relative distribution of miRNAs within each sample was reasonably consistent as RNA
265 input decreased. However, some miRNA species tended to be over-represented at the lowest
266 mitochondria RNA inputs. This may be because there were less miRNA species detected in the library
267 prepared from 1.8 ng (207 miRNAs) when compared to 60 ng mitochondria RNA (266 miRNAs).
268 Overall, there appears to be minimal bias towards over- or under-representing specific miRNA species
269 at low RNA inputs.

270 Of note, the skeletal muscle-enriched miR-1, miR-133a and miR-133b were detected at high (30 and
271 60 ng) but not low (1.8-15 ng) mitochondrial RNA inputs. MiR-1 and miR-133a have previously been
272 observed in mitochondria isolated from human skeletal and rodent cardiac muscle cells *in vitro* (Barrey
273 et al., 2011, Jagannathan et al., 2015, Zhang et al., 2014). MiR-1 enhances the transcription of the
274 mitochondrial-encoded *Mt-co1, Mt-nd1* and *Mt-cytb*, among others (Zhang et al., 2014), while miR-
275 133a inhibits the transcription of nuclear-encoded genes including *Ppargc1a* and *Tfam* (Nie et al.,
276 2016), both of which are upstream regulators of mitochondrial biogenesis. The use of proliferating L6
277 myocytes in this study, compared with primary human myocytes (Barrey et al., 2011) and rat neonatal
278 cardiomyocytes (Zhang et al., 2014) used previously, may partially account for the differences in
279 miRNA species detected. Although L6 cells have reportedly higher rates of aerobic metabolism when
280 compared to C2C12 cells and primary human myocytes, cell culture models are more dependent upon
281 anaerobic glycolysis (Abdelmoez et al., 2020). Thus, mitochondrial abundance and function in various
282 cell culture models may differ to those observed with *in vivo* models. This study was primarily designed
283 to optimise the sRNA-Seq library preparation protocol rather than investigate the physiological
284 relevance of specific miRNAs. Future *in vivo* studies are now required to profile mitochondrial miRNAs
285 and their roles in tissues that have high bioenergetic requirements such as skeletal and cardiac muscle.

286 Finally, having a reliable method to discover nuclear-encoded RNAs within mitochondria in response
287 to physiological stimuli will allow for future studies into RNA import and/or regulation at the

288 subcellular level. For instance, non-coding RNAs such as lncRNAs can have important regulatory roles
289 (Wadley et al., 2019), mediating cellular processes by modulating the expression of genes, stability of
290 transcripts and/or function of proteins (Long et al., 2017), including those that directly determine
291 mitochondrial function. However, only a relatively small fraction (~5-10%) of all identified lncRNAs
292 have been functionally characterized (Gao et al., 2020). Therefore, understanding the subcellular
293 distribution may also open new avenues of investigation into how they are imported into the
294 mitochondrial compartment, what are their putative binding target(s) and whether they modulate
295 expression levels of mtDNA encoded genes and/or function of mitochondrial proteins. This will be key
296 to understanding the potential effects on mitochondrial parameters such as oxidative phosphorylation,
297 ROS production, mitochondrial biogenesis, dynamics or mitophagy.

298 In summary, we report a method for obtaining a highly pure fraction of mitochondria from cultured
299 myoblasts and skeletal muscle tissue and optimised approach for high throughput transcriptomic
300 sequencing on this subcellular fraction. Given the increasing interest in RNA-mediated regulation of
301 cellular function in health and disease, future investigations are warranted to better understand the
302 potential biological and physiological significance of the mitochondrial localisation of nuclear-encoded
303 RNAs.

304

305 **MATERIALS AND METHODS**

306 Cell culture

307 L6 rat myoblast cells were obtained from a commercial vendor (ATCC Cat# CRL-1458, RRID:
308 CVCL_0385). Cells were cultured at 37°C with 5% CO_2 in a humidified incubator in media consisting
309 of Dulbecco's Modified Eagle Medium (DMEM; Gibco #11995-065) supplemented with 10% v/v FBS
310 (Gibco #A3161001), 100 U/ml penicillin and 100 µg/ml streptomycin (Gibco #15140-122). Cells were
311 grown in 150 mm dishes to ~90% confluence then washed with sterile PBS and detached (Gibco
312 TrypLE Express #LTS12604021). Cells used for all experiments were ≤9 passages from stock and
313 tested negative for mycoplasma contamination (Agilent MycoSensor QPCR Assay Kit, 302107).

314 Myoblast mitochondrial isolation

315 Mitochondria were isolated from L6 myoblasts via immunoprecipitation (Miltenyi Biotek #130-096-
316 946). Briefly, ~$5x10^6$ cells (suspended in a small volume of PBS after detachment) were transferred to
317 1 mL ice-cold lysis buffer on ice, then mechanically homogenised with 20 passes in a 7 mL glass dounce
318 homogeniser (#357542, Wheaton, NJ). Wash buffer (9 mL) was added to the lysate and transferred to
319 a falcon tube. Anti-TOMM22 antibody conjugated magnetic beads (50 µL) were added to the 10 mL
320 lysate and incubated with gentle inversion for 1 hour at 4°C. Lysate was passed through a pre-separation
321 filter then flowed through a column mounted on a magnetic rack. Mitochondria were washed 3 times

322 prior to elution. Mitochondria were pelleted via centrifugation at 13,000 x g for 2 minutes at 4°C.
323 Supernatant was then removed and the mitochondrial pellet resuspended in storage buffer to be used
324 for subsequent enzymatic purification steps described below.

325 Enzymatic purification of myoblast mitochondria

326 Protease treatment: To remove proteins not localised within intact mitochondria, aliquots of isolated
327 mitochondria (1 µg total protein each) were incubated in a 50 µL reaction with or without triton-x (1%
328 v/v) and with or without proteinase K (Qiagen #19131, final concentration 20 µg/mL) for 15 minutes
329 at room temperature. Phenylmethylsulfonyl fluoride (20 mM) was added to inhibit proteinase-K.
330 Samples were then stored at -20°C until immunoblot analysis.

331 RNase treatment: To remove RNA not localised within intact mitochondria, in a 50 µL reaction, aliquots
332 of isolated mitochondria (1 µg total protein each) first had 100 ng mRNA spike-in control added
333 (StemMACS eGFP mRNA #130-101-114, Miltenyi Biotec), and were then incubated with or without
334 triton-x (1% v/v) and with or without Rnase-A (Qiagen #19101, final concentration range 1-1000
335 µg/mL) and incubated on ice for 30 minutes. Trizol reagent was then added to simultaneously inactivate
336 Rnase activity, lyse mitochondria and preserve RNA. Samples were then stored in Trizol at -20°C until
337 RNA isolation.

338 Immunoblot analysis

339 Mitochondrial samples were resuspended in RIPA buffer (Millipore #20-188) containing protease
340 inhibitors (Sigma #P8340). Protein concentration was determined by BCA assay (Pierce #23225).
341 Samples were mixed with reducing loading buffer (4x Laemmli sample buffer with 10% 2-
342 mercaptoethanol). Samples were loaded into a 4-15% gel (Bio-Rad #5678085) in addition to molecular
343 weight marker (Bio-Rad #161-0373), which were then separated by electrophoresis. The stain-free gel
344 was UV-activated for 1 minute and imaged for total protein (BioRad Chemi Doc XR+, Hercules, CA,
345 USA) with ImageLab software (BioRad Image Lab v6). Protein was then transferred to a methanol
346 soaked polyvinylidene difluoride (PVDF) membrane (Millipore Immobilon FL 0.45 µm #IPFL00010).
347 The membrane was then PBS washed, then blocked for 1 hour (Li-Cor Intercept PBS blocking buffer).
348 The membrane was then incubated with primary antibody in blocking buffer + 0.2% v/v Tween-20
349 overnight at 4°C. Primary antibodies used were: anti-TOMM20 (Abcam #ab186735; 1:1000), anti-
350 Cytochrome-c (Abcam #ab133504; 1:1000), anti-Citrate Synthase (Cell Signaling Technology #14309;
351 1:1000), anti-α-Tubulin (Cell Signaling Technology #3873; 1:1000), anti-mitofilin (Abcam #ab110329;
352 1:1000), anti-AIF (Cell Signaling Technology #4642, 1:500), (anti-catalase (Abcam #ab1877, 1:500),
353 anti-S6 RPL (Cell Signaling Technology #2217, 1:1000), anti-GM130 (BD Transduction Laboratories
354 #610822, 1:1000), anti-SERCA1 (Cell Signaling Technology #4219, 1:1000), and anti-Lamin B1 (Cell
355 Signaling Technology #12586; 1:1000). Membranes were then washed with PBST and incubated with

356 secondary antibodies (Cell Signaling Technology) anti-rabbit or anti-mouse IgG Dylight® 680 nm (Cell
357 Signaling Technology #5366S, #5470S) or 800 nm (Cell Signaling Technology #5151S or #5257S) at
358 1:10,000 in blocking buffer containing 0.2% Tween-20 and 0.01% SDS for 1 hour at room temperature.
359 Fluorescent signal was then digitally acquired (Licor Odyssey® Infrared Imaging System, Lincoln, NE,
360 USA).

361 RNA isolation and quality control

362 Myoblast mitochondria samples stored in Trizol were thawed on ice and centrifuged at 10,000 x g for
363 10 min at 4°C. An aliquot of the supernatant was then used for RNA purification with on-column
364 DNase-I treatment (Direct-Zol RNA Microprep R2060, Zymo Research). RNA concentration and
365 purity was determined by spectrophotometry (NanoDrop 1000, Thermo Fisher Scientific) while RNA
366 fragment size distribution was assessed by gel electrophoresis (Tapestation HS-RNA, Agilent
367 Technologies).

368 Reverse transcription and quantitative PCR (RT-qPCR)

369 Equal volumes of isolated RNA from the RNase-treated mitochondria samples (to account for
370 differences in total RNA yield between samples due to RNase treatment) were reverse transcribed to
371 first-strand cDNA in a 20 µL reaction along with no-template and no-RTase controls (Applied
372 Biosystems High Capacity RT kit #4368814). Quantitative PCR was performed in triplicate (Agilent
373 AriaMX G8830A) on 4 ng of cDNA in a 10 µL reaction consisting of SYBR green master mix (Applied
374 Biosystems #4367659) with 0.3 µM forward and reverse primers (Table 1).

Table 1. List of RT qPCR primers

Target	Forward (5' -3')	Reverse (5' -3')	Accession ID
Mt-co3	GACGGAATTTACGGCTCAACAT	AATTAGGAAAGTTGAGCCAATAATTACG	>NC_001665.2 Rattus norvegicus strain BN/SsNHsdMCW mitochondrion, complete genome
Cox4i1	GTGCTGATCTGGGAGAAGAGCTA	GGTTGACCTTCATGTCCAGCAT	>NM_017202.1 Rattus norvegicus cytochrome c oxidase subunit 4i1 (*Cox4i1*), mRNA; nuclear gene for mitochondrial product
eGFP	ACTTCTTCAAGTCCGCCATG	AGCTCGATGCGGTTCACCAG	>XM_013480425.1 Eimer ia maxima Green fluorescent protein, related partial mRNA

375

376 Thermal conditions used for qPCR were 10 min at 95°C (activation) then 40 cycles of 15 s at 95°C
377 (denature) and 60 s at 55-60°C (anneal/extend). A dissociation curve was performed to confirm the

378 amplification of a single product. Quantification cycle (C_q) thresholds were calculated using software
379 (Agilent Aria v1.5).

380

381 Myoblast small RNA sequencing and bioinformatics

382 Total RNA isolated from individual (*n*=7) L6 mitochondria samples was pooled into a single tube, from
383 which serial dilutions ranging from 0.3-20 ng/µL were prepared. cDNA libraries were then prepared
384 using a range of mitochondrial RNA inputs (final input range 1.8-120 ng) using the NEBNext Multiplex
385 Small RNA Library Prep Set (New England Biolabs). To investigate the efficiency of small RNA library
386 preparation across a range of mitochondrial RNA inputs, libraries were prepared either according to the
387 manufacturer's recommendations for low RNA inputs (NEBNext 3´ and 5' SR Adaptors, and RT primer
388 for Ilumina diluted 0.5X, 15 PCR cycles) or with modifications (NEBNext 3´ and 5' SR Adaptors, and
389 RT primer for Ilumina diluted 0.3X or 0.1X, 20 PCR cycles). cDNA concentration was determined by
390 fluorometric quantitation (Qubit 1xdsDNA, Thermo Fisher Scientific) while cDNA fragment size
391 distribution was assessed by gel electrophoresis (Tapestation HS-D1000, Agilent Technologies).

392 An equimolar pool of all uniquely indexed small RNA libraries was prepared. Twenty-five µL of the
393 equimolar pool was loaded across two lanes on a 6% Novex TBE polyacrylamide gel (Thermo Fischer
394 Scientific), with 5 µL Quick-Load pBR322 DNA-MspI Molecular Marker (New England Biolabs Inc.)
395 in a separate lane. The buffer dam was filled with 600 mL 1X TBE running buffer and the gel run at
396 120V for 1h. The gel was then incubated with 50 mL 1X TBE spiked with 1X SYBR Gold Nucleic
397 Acid Gel Stain (Thermo Fischer Scientific), before being visualised on a Safe Imager 2.0 Blue-Light
398 Transilluminator (Invitrogen) following exposure to UV-Blue (470 nm) light. Fragments corresponding
399 to the 130-160 bp region were manually excised, before suspended and then crushed in 250 µL gel
400 elution buffer (New England Biolabs Inc.). To increase the recovery of low concentrations of small
401 nucleic acids, cDNA was precipitated overnight at -20°C with 0.3 M sodium acetate (pH 5.5), 4X
402 volumes of 100% ethanol and 1 µL linear acrylamide carrier. Following overnight precipitation, the
403 solution was centrifuged at 16,000x*g* for 60 minutes to pellet the cDNA fragment. The cDNA pellet
404 was washed twice with 80% ethanol and resuspend in 12 µL TE buffer. Fragment size distribution of
405 the gel-extracted cDNA pool was assessed by gel electrophoresis (Tapestation HS-D1000, Agilent
406 Technologies).

407 RNA sequencing was performed by the Deakin University Genomics Core on the Illumina MiniSeq
408 platform. A 1.3 pM loading pool was prepared with 20% Phi-X spike-in and was sequenced on a single-
409 end 75 bp run. Sequenced reads underwent quality checks with FastQC before the adapter and reads
410 <20nt were trimmed. Small RNAs, including miRNAs, are not well sequenced in the rat genome but
411 are conserved between rat and mouse species. Reads were mapped to known mature mouse miRNAs

412 accessible from miRbase v22.0. Raw read counts were normalised by the size of each individual library.
413 Counts were visualised using GraphPad Prism (v7).

414

415 Rodent study ethical approval and procedures

416 All experimental procedures were approved by the Deakin University Animal Ethics Committee (G02-
417 2019). All animals were housed and treated in accordance with standards set by Deakin University's
418 Animal Welfare Committee, which complies with the ethical and governing principles outlined in the
419 Australian code for the care and use of animals for scientific purposes. Wistar Kyoto male rats were
420 obtained from the Animal Resource Centre, Perth, Western Australia. Rats were housed in pairs and
421 maintained with a 12-hour light/dark cycle, constant temperature of 21 ± 2°C, and humidity levels
422 between 40 and 70%. Rats had *ad libitum* access to standard chow diet and tap water. At 9-weeks of
423 age, animals were humanely killed following dissection of the heart under heavy anaesthesia using 5%
424 isoflurane gas. The gastrocnemius muscle was rapidly excised then the inner red portion was dissected.
425 A portion of this was snap frozen in liquid nitrogen for subsequent whole muscle RNA analyses, and a
426 separate ~ 100 mg piece was taken for mitochondrial isolation.

427

428 Rat muscle tissue mitochondrial isolation

429 Tissue was immediately placed in 1 mL ice-cold lysis buffer containing 5 µl/ml protease inhibitors
430 (Sigma #P8340) and minced using fine scissors before mechanical homogenisation with an ice-cold
431 Teflon-tipped glass dounce homogeniser (10 passes with rotation at 350 rpm). Intact mitochondria were
432 then isolated using the magnetic-bead immunoprecipitation method as described above for L6
433 myoblasts except with the following RNase treatment conditions: RNase-A 340 µg/mL in a reaction
434 with ~20 µg total mitochondrial protein performed for 1 hour at 37°C, after which 5 µL proteinase-K
435 (stock concentration 600 mAU/mL) was then added to inactivate RNase activity (Barrey et al., 2011).
436 Each tube was briefly inverted before the mitochondria solutions were then centrifuged at 8000 x g for
437 10 min at 4°C. The supernatant was aspirated and the pellet was washed twice with 100 µL ice-cold
438 storage buffer. The RNase-treated mitochondrial pellet was resuspended in 100 uL storage buffer then
439 frozen at -80°C until RNA extraction.

440 Rat muscle tissue and isolated mitochondria RNA extraction

441 For RNA extraction from gastrocnemius whole muscle tissue, ~15 mg frozen tissue was placed in a
442 liquid nitrogen pre-chilled cyrotube with a 5 mm stainless steel bead. The tissue was then mechanically
443 disrupted (2 cycles at 4m/s for 10 s, MP Biomedical FastPrep). Tri-reagent (600 uL) was added, then
444 RNA extracted (Zymo DirectZol RNA Miniprep #R2050). For RNA extraction from isolated

445 mitochondria from the respective red portion of gastrocnemius muscle, frozen samples were thawed in
446 the presence of 5 volumes of TRI-reagent (Qiagen), pipette mixed thoroughly then centrifuged at 16,000
447 x g for 1 min. RNA extraction was then performed with on-column DNase I treatment (Zymo Research
448 DirectZol RNA Microprep #2060). Extracted RNA was tested for purity on Nanodrop, concentration
449 with Qubit HS RNA assay (Thermo Fisher) then RNA integrity number (RIN) was determined using a
450 Tapestation (Agilent) with High Sensitivity RNA reagents. All RINs from whole tissue RNA were ≥7.0.

451 Rat muscle tissue and isolated mitochondria total RNA sequencing

452 Total RNA from whole-tissue (50 ng) and isolated mitochondria (10 ng) were converted to cDNA
453 libraries (Zymo-Seq RiboFree Total RNA #R300, Zymo Research). Briefly, ribosomal RNA was
454 depleted, then remaining transcripts were fragmented and converted to cDNA using random priming.
455 After second strand synthesis, the ends of the cDNA were enzymatically repaired and Illumina-
456 compatible sequencing adaptors were ligated. Library size (TapeStation, Agilent) and concentration
457 (Qubit) was assessed prior to sequencing. RNA sequencing was performed by the Deakin University
458 Genomics Core on the Illumina NovaSeq 6000 platform. Reads underwent adapter trimming and quality
459 check with Skewer then mapped to the rat genome (Ensembl version 99) with STAR aligner v2.7.2a.
460 STAR generated read counts were collated in R version 4.0.3 (R Development Core Team, 2010).
461 Normalised counts were visualised using GraphPad Prism (v7). Analysis of differential expression was
462 performed using Voom/Limma in Degust v 4.1.5 (Powell, 2019). Transcripts with a false discovery rate
463 (FDR) <0.05 were considered differentially expressed.

464

465 Rat muscle tissue mitoplast preparation and RNA sequencing

466 All experimental procedures were approved by the Deakin University Animal Ethics Committee (G01-
467 2023) and housed and treated in accordance with standards set by Deakin University's Animal Welfare
468 Committee, which complies with the ethical and governing principles outlined in the Australian code
469 for the care and use of animals for scientific purposes. A 14 week old male Wistar Kyoto rat was
470 obtained from the Animal Resource Centre, Perth, Western Australia and humanely killed following
471 dissection of the heart under heavy anaesthesia using 5% isoflurane gas. The hindlimb muscles were
472 rapidly excised and cut into 200 mg pieces. Each piece was immediately placed in 1 mL ice-cold lysis
473 buffer containing 5ul/ml protease inhibitors (Sigma #P8340), minced using fine scissors and incubated
474 on ice for 30 min. Samples were then mechanically homogenised with an ice-cold Teflon-tipped glass
475 dounce homogeniser (10 passes with rotation at 350 rpm) and the homogenate was pooled. To compare
476 different isolation methods, intact mitochondria were then isolated from separate aliquots of the same
477 homogenate using either the magnetic-bead immunoprecipitation method described above, or a
478 differential centrifugation method.

479 To obtain mitochondria by differential centrifugation, tissue homogenate was spun at 800 × g for 10
480 min at 4°C and the pellet was discarded. The supernatant was then spun at 16,000 × g for 30 min at 4°C
481 and the pellet resuspended in 1 mL of isolation buffer containing 1mM PMSF and then spun at 10,000
482 × g for 10 mins at 4°C. The mitochondrial pellets were washed twice in 1 mL ice-cold storage buffer.
483 The mitochondrial pellets were then pooled and resuspended a small volume of storage buffer.

484 To generate mitoplasts, intact mitochondria (40 µg) obtained from the magnetic-bead
485 immunoprecipitation method were incubated in 0.06% digitonin on ice for 30 min, followed by 30 min
486 incubation on ice with proteinase-K (final concentration 20 µg/mL). The samples were then incubated
487 on ice for 10 min in PMSF (final concentration 10 mM) to inhibit proteinase-K. The mitoplast pellets
488 were then washed once in 0.75 mL storage buffer containing 5 mM PMSF and then once in 0.75 mL
489 storage buffer without PMSF. Each time the pellets were spun at 13,000 × g for 2 min at 4°C and the
490 supernatants discarded. Finally, the mitoplast pellets were resuspended in 40 µL storage buffer.

491 The following 4 different treatments were conducted in triplicate on 40 µg of protein from mitochondria
492 or mitoplasts that were obtained from the hindlimb muscle of a single animal. All four treatments
493 included 120 µg/mL RNase-A (cat# 19101, Qiagen, Hilden, Germany) incubation for 30 min on ice.

494 1. MitoProK: Mitochondria from magnetic-bead IP, +RNase-A (followed by 20 µg/mL proteinase-K)
495 2. MitoRNase: Mitochondria from magnetic-bead IP, +RNase-A (no proteinase-K)
496 3. MitoplastRNase: Mitoplasts, +RNase-A (no proteinase-K)
497 4. CrudeMito: Mitochondria from differential centrifugation, +RNase-A (no proteinase-K)

498 After RNase-A incubation, either proteinase-K (final concentration 20 µg/mL) or a similar volume of
499 buffer was added to the respective treatment groups and incubated on ice for 30 min. Each tube was
500 then centrifuged at 13,000 × g for 2 min at 4°C. The supernatant was aspirated and the pellet was washed
501 once with 500 µL and then once with 200 µL ice-cold storage buffer. The mitochondrial pellets were
502 resuspended in 400 µL Tri-reagent and frozen at -80°C until RNA extraction.

503 For RNA extraction, frozen samples were thawed and then pipette mixed thoroughly to disrupt the
504 pellets and then centrifuged at 13,000 x g for 10 min. RNA extraction was then performed with on-
505 column DNase I treatment (Zymo Research DirectZol RNA Microprep #2060) and eluted in 12 µL
506 nuclease free water. RNA yield was determined using a Tapestation (Agilent) with High Sensitivity
507 RNA reagents. Mitochondria from magnetic-bead IP yielded ~1.5 ng RNA per µg of protein, whereas
508 mitochondria from differential centrifugation yielded ~0.2 ng RNA per µg of protein.

509 Total RNA extracted from mitochondria from differential centrifugation (6.3 ng), mitochondria and
510 mitoplasts isolated from magnetic-bead IP (40 ng) methods were converted to cDNA libraries (Zymo-
511 Seq RiboFree Total RNA #R300, Zymo Research) then underwent whole transcriptome RNA
512 sequencing as described above.

513 Statistical analysis

514 Small RNA-seq data was analysed by paired t-test. RNase-A dose-response data were tested for
515 normality of variance and then analysed by one- or two-way ANOVA with Tukey's post hoc test for
516 multiple comparisons using GraphPad Prism (v7). All data are presented as mean (SD) with significance
517 accepted at $p<0.05$.

518 **Acknowledgments**

519 We acknowledge Gisella Mazzarino and Amandi Gunawardena for their assistance with animal
520 experiments and tissue collection and Erin Mayne for her assistance with the muscle tissue mitoplast
521 preparation and RNA sequencing experiments. We acknowledge Sarah Alexander for her assistance
522 with female participant recruitment. Severine Lamon is supported by an Australian Research Council
523 Future Fellowship (FT10100278).

524 **Author contributions**

525 Conceptualization: JLS, AJT, SN, S.Lamon, GDW
526 Conducted experiments: JLS, AJT, GDW, S.Loke
527 Conducted human studies: JLS, GDW, S.Lamon, HD
528 Data analysis (bioinformatics): MZ, LC, MS
529 Data analysis and visualisation: JLS, AJT, MS
530 Manuscript – original draft: JLS & AJT
531 Manuscript– review and editing: all authors.
532 Approved final version of manuscript: all authors.
533
534

535 **REFERENCES**

536

537 ABDELMOEZ, A. M., SARDÓN PUIG, L., SMITH, J. A. B., GABRIEL, B. M., SAVIKJ, M., DOLLET, L.,
538 CHIBALIN, A. V., KROOK, A., ZIERATH, J. R. & PILLON, N. J. 2020. Comparative profiling of
539 skeletal muscle models reveals heterogeneity of transcriptome and metabolism. *Am J Physiol*
540 *Cell Physiol,* 318**,** C615-c626.
541 BANDIERA, S., RUBERG, S., GIRARD, M., CAGNARD, N., HANEIN, S., CHRETIEN, D., MUNNICH, A.,
542 LYONNET, S. & HENRION-CAUDE, A. 2011. Nuclear outsourcing of RNA interference
543 components to human mitochondria. *PLoS One,* 6**,** e20746.
544 BARREY, E., SAINT-AURET, G., BONNAMY, B., DAMAS, D., BOYER, O. & GIDROL, X. 2011. Pre-microRNA
545 and mature microRNA in human mitochondria. *PLoS One,* 6**,** e20220.
546 DAS, S., FERLITO, M., KENT, O. A., FOX-TALBOT, K., WANG, R., LIU, D., RAGHAVACHARI, N., YANG, Y.,
547 WHEELAN, S. J., MURPHY, E. & STEENBERGEN, C. 2012. Nuclear miRNA regulates the
548 mitochondrial genome in the heart. *Circ Res,* 110**,** 1596-603.
549 DASGUPTA, N., PENG, Y., TAN, Z., CIRAOLO, G., WANG, D. & LI, R. 2015. miRNAs in mtDNA-less cell
550 mitochondria. *Cell Death Discov,* 1**,** 15004.
551 GAO, F., CAI, Y., KAPRANOV, P. & XU, D. 2020. Reverse-genetics studies of lncRNAs—what we have
552 learnt and paths forward. *Genome Biology,* 21**,** 93.
553 GOLD, V. A., CHROSCICKI, P., BRAGOSZEWSKI, P. & CHACINSKA, A. 2017. Visualization of cytosolic
554 ribosomes on the surface of mitochondria by electron cryo-tomography. *EMBO Rep,* 18**,** 1786-
555 1800.
556 JAGANNATHAN, R., THAPA, D., NICHOLS, C. E., SHEPHERD, D. L., STRICKER, J. C., CROSTON, T. L.,
557 BASELER, W. A., LEWIS, S. E., MARTINEZ, I. & HOLLANDER, J. M. 2015. Translational Regulation
558 of the Mitochondrial Genome Following Redistribution of Mitochondrial MicroRNA (MitomiR)
559 in the Diabetic Heart. *Circulation. Cardiovascular genetics,* 8**,** 785-802.
560 LONG, Y., WANG, X., YOUMANS, D. T. & CECH, T. R. 2017. How do lncRNAs regulate transcription?
561 *Science Adv,* 3**,** eaao2110.
562 LUNG, B., ZEMANN, A., MADEJ, M. J., SCHUELKE, M., TECHRITZ, S., RUF, S., BOCK, R. & HUTTENHOFER,
563 A. 2006. Identification of small non-coding RNAs from mitochondria and chloroplasts. *Nucleic*
564 *Acids Res,* 34**,** 3842-52.
565 MERCER, T. R., NEPH, S., DINGER, M. E., CRAWFORD, J., SMITH, M. A., SHEARWOOD, A. M., HAUGEN,
566 E., BRACKEN, C. P., RACKHAM, O., STAMATOYANNOPOULOS, J. A., FILIPOVSKA, A. & MATTICK,
567 J. S. 2011. The human mitochondrial transcriptome. *Cell,* 146**,** 645-58.
568 NIE, Y., SATO, Y., WANG, C., YUE, F., KUANG, S. & GAVIN, T. P. 2016. Impaired exercise tolerance,
569 mitochondrial biogenesis, and muscle fiber maintenance in miR-133a-deficient mice. *Faseb j,*
570 30**,** 3745-3758.
571 NIELSEN, S., SCHEELE, C., YFANTI, C., AKERSTROM, T., NIELSEN, A. R., PEDERSEN, B. K. & LAYE, M. J.
572 2010. Muscle specific microRNAs are regulated by endurance exercise in human skeletal
573 muscle. *J Physiol,* 588**,** 4029-37.
574 NOH, J. H., KIM, K. M., ABDELMOHSEN, K., YOON, J.-H., PANDA, A. C., MUNK, R., KIM, J., CURTIS, J.,
575 MOAD, C. A. & WOHLER, C. M. 2016. HuR and GRSF1 modulate the nuclear export and
576 mitochondrial localization of the lncRNA RMRP. *Genes Dev,* 30**,** 1224-1239.
577 POWELL, D. 2019. Degust v4.1.1. Zenodo. doi.org/10.5281/zenodo.3501067.
578 RAJKUMAR, A. P., QVIST, P., LAZARUS, R., LESCAI, F., JU, J., NYEGAARD, M., MORS, O., BØRGLUM, A.
579 D., LI, Q. & CHRISTENSEN, J. H. 2015. Experimental validation of methods for differential gene
580 expression analysis and sample pooling in RNA-seq. *BMC Genomics,* 16**,** 548.
581 RUSSELL, A. P., FOLETTA, V. C., SNOW, R. J. & WADLEY, G. D. 2014. Skeletal muscle mitochondria: a
582 major player in exercise, health and disease. *Biochim Biophys Acta,* 1840**,** 1276-84.

583 RUSSELL, A. P., LAMON, S., BOON, H., WADA, S., GULLER, I., BROWN, E. L., CHIBALIN, A. V., ZIERATH,
584 J. R., SNOW, R. J., STEPTO, N., WADLEY, G. D. & AKIMOTO, T. 2013. Regulation of miRNAs in
585 human skeletal muscle following acute endurance exercise and short-term endurance
586 training. *J Physiol,* 591**,** 4637-53.
587 SHORE, S., HENDERSON, J. M., LEBEDEV, A., SALCEDO, M. P., ZON, G., MCCAFFREY, A. P., PAUL, N. &
588 HOGREFE, R. I. 2016. Small RNA Library Preparation Method for Next-Generation Sequencing
589 Using Chemical Modifications to Prevent Adapter Dimer Formation. *PLoS One,* 11**,** e0167009.
590 SILVER, J., WADLEY, G. & LAMON, S. 2018. Mitochondrial regulation in skeletal muscle: A role for non-
591 coding RNAs? *Experimental Physiology* 103**,** 1132-1144.
592 SPINELLI, J. B. & HAIGIS, M. C. 2018. The multifaceted contributions of mitochondria to cellular
593 metabolism. *Nat Cell Biol,* 20**,** 745-754.
594 SRIPADA, L., TOMAR, D., PRAJAPATI, P., SINGH, R., SINGH, A. K. & SINGH, R. 2012. Systematic Analysis
595 of Small RNAs Associated with Human Mitochondria by Deep Sequencing: Detailed Analysis
596 of Mitochondrial Associated miRNA. *PLoS ONE,* 7**,** e44873.
597 SUISSA, M. & SCHATZ, G. 1982. Import of proteins into mitochondria. Translatable mRNAs for
598 imported mitochondrial proteins are present in free as well as mitochondria-bound
599 cytoplasmic polysomes. *J Biol Chem,* 257**,** 13048-55.
600 TAKELE ASSEFA, A., VANDESOMPELE, J. & THAS, O. 2020. On the utility of RNA sample pooling to
601 optimize cost and statistical power in RNA sequencing experiments. *BMC Genomics,* 21**,** 312.
602 WADLEY, G. D., LAMON, S., ALEXANDER, S. E., MCMULLEN, J. R. & BERNARDO, B. C. 2019. Non-coding
603 RNAs regulating cardiac muscle mass. *Journal of Applied Physiology,* 127**,** 633-644.
604 WANG, G., CHEN, H. W., OKTAY, Y., ZHANG, J., ALLEN, E. L., SMITH, G. M., FAN, K. C., HONG, J. S.,
605 FRENCH, S. W., MCCAFFERY, J. M., LIGHTOWLERS, R. N., MORSE, H. C., 3RD, KOEHLER, C. M.
606 & TEITELL, M. A. 2010. PNPASE regulates RNA import into mitochondria. *Cell,* 142**,** 456-67.
607 WANG, X., SONG, C., ZHOU, X., HAN, X., LI, J., WANG, Z., SHANG, H., LIU, Y. & CAO, H. 2017.
608 Mitochondria Associated MicroRNA Expression Profiling of Heart Failure. *Biomed Res Int,*
609 2017**,** 4042509.
610 WITZEL, H. 1963. The Function of the Pyrimidine Base in the Ribonuclease Reaction. *In:* DAVIDSON, J.
611 N. & COHN, W. E. (eds.) *Progress in Nucleic Acid Research and Molecular Biology.* Academic
612 Press.
613 ZHANG, X., ZUO, X., YANG, B., LI, Z., XUE, Y., ZHOU, Y., HUANG, J., ZHAO, X., ZHOU, J., YAN, Y., ZHANG,
614 H., GUO, P., SUN, H., GUO, L., ZHANG, Y. & FU, X. D. 2014. MicroRNA directly enhances
615 mitochondrial translation during muscle differentiation. *Cell,* 158**,** 607-19.
616 ZURLO, F., LARSON, K., BOGARDUS, C. & RAVUSSIN, E. 1990. Skeletal muscle metabolism is a major
617 determinant of resting energy expenditure. *J Clin Invest,* 86**,** 1423-7.

618

619

620

621 **FIGURE LEGENDS**

622 **Figure 1. Overview of TOMM22 immunoprecipitation based method for mitochondrial isolation**

623

624 **Figure 2. Protease treatment of mitochondria isolated from L6 myocytes.** Isolated mitochondria
625 were incubated with or without proteinase-K (20 µg/mL) and detergent (1% triton-X). Mitochondria
626 (0.2 µg total protein) and whole cell lysate (12 µg total protein) were resolved via SDS-PAGE and
627 probed for marker proteins of subcellular compartments: TOMM20 (OMM), Cytochrome-c (IMS),
628 citrate synthase (matrix), α-tubulin (cytosol), lamin B1 (nucleus). Blots are representative of *n*=2
629 technical replicates from a single mitochondrial isolation preparation.

630

631 **Figure 3. RNase-A treatment of mitochondria isolated from L6 myocytes.** Isolated mitochondria
632 were incubated with or without RNase-A (1-1000 µg/mL) in the presence or absence of detergent (1%
633 triton-X). The levels of representative mtDNA (*Mtco3*) and nuclear (*Cox4i1*) encoded genes were then
634 assessed by RT-qPCR in addition to an exogenous mRNA spike-in control (*eGFP*) added to isolated
635 mitochondria (but not to the whole cell lysate). Data are mean(SD) for *N*=3 technical replicates from a
636 single mitochondrial isolation preparation.

637

638 **Figure 4. Small RNA-Seq on isolated mitochondria from L6 myocytes. A)** Small RNA libraries
639 were prepared from 1.8 to 60 ng mitochondria RNA with modified-0.3X (n=6) or modified-0.1X (*n*=4)
640 protocols. The total number of reads (*p*=0.79) and total mapped miRNA reads (*p*=0.19) were not
641 different between protocols. Student's paired t-test, *n*=1 at each RNA input. **B)** Neither mitochondrial
642 RNA input nor library preparation protocols limit the number of mature miRNAs that can be detected
643 from mitochondrial RNA. The number of mature miRNA species detected across all mitochondria RNA
644 inputs was not different (*p*=0.60, student's paired t-test) following modified-0.3X (m-0.3X; *n*=6) and
645 modified-0.1X (m-0.1X; *n*=4) protocols. Each point represents an independent library prepared from
646 1.8-60 ng mitochondrial RNA. **C-E)** The relative abundance of miRNAs within each sample is
647 comparable between small RNA libraries prepared from high, moderate and low mitochondrial RNA
648 inputs. Venn diagrams depicting unique and shared miRNAs detected from 60 ng mitochondria RNA
649 when compared to **C)** 1.8 ng, **D)** 7.5 ng and **E)** 30 ng mitochondria RNA, prepared using the modified-
650 0.3X library preparation approach. The relative distribution of miRNAs detected at each RNA input
651 was expressed relative to miR-let-7c-2. Differences in the relative distribution of miRNAs between the
652 highest RNA input and serial RNA dilutions are depicted by grey dots (<5-fold change when compared
653 to 60ng), red dots (>5-fold change when compared to 60ng) and green dots (>10-fold change when

654 compared to 60ng). Highly abundant miRNAs across all RNA inputs (including the let-7 family and
655 mmu-miR-206) are shown in orange dots.

656

657 **Figure 5. Mitoplasts and enzymatically-treated isolated mitochondria from rat skeletal muscle**
658 **tissue have a similar RNA transcriptome. A)** PCA plot of RNA-seq whole transcriptome of
659 mitochondria isolated via IP, RNase-A treated, then treated with proteinase-K ("MitoRnase+ProtK") or
660 without ("MitoRnase"), mitoplast preparations treated with RNase-A ("MitoplastRnase"), and crude
661 mitochondria extracts isolated by differential centrifugation treated with RNase-A ("CrudeMito"). Data
662 are N=3 technical replicates (independent mitochondrial isolation procedures), from the tissue of n=1
663 animal. Volcano plots of differentially expressed **B)** mtDNA encoded genes, and **C)** nuclear-encoded
664 genes between the different mitochondrial treatments and mitoplasts, statistical significance accepted
665 at adjusted p-value (FDR) <0.05 and $\log_2$ fold-change <1.

666

667 **Figure 6. Purity of enzymatically-treated isolated mitochondria from rat skeletal muscle relative**
668 **to respective whole muscle tissue. A)** Whole-transcriptome RNA sequencing of isolated mitochondria
669 and respective whole muscle tissue (rat gastrocnemius) shows that the isolated mitochondria were free
670 of **D)** highly abundant muscle sarcomere related mRNAs **B)** and nuclear-encoded mRNAs involved in
671 the mitochondrial electron transport chain, while **C)** mtDNA encoded mitochondrial electron transport
672 chain genes were present. Each point represents the mean normalised abundance (counts per million,
673 CPM) of an individual gene from n=6 animals.

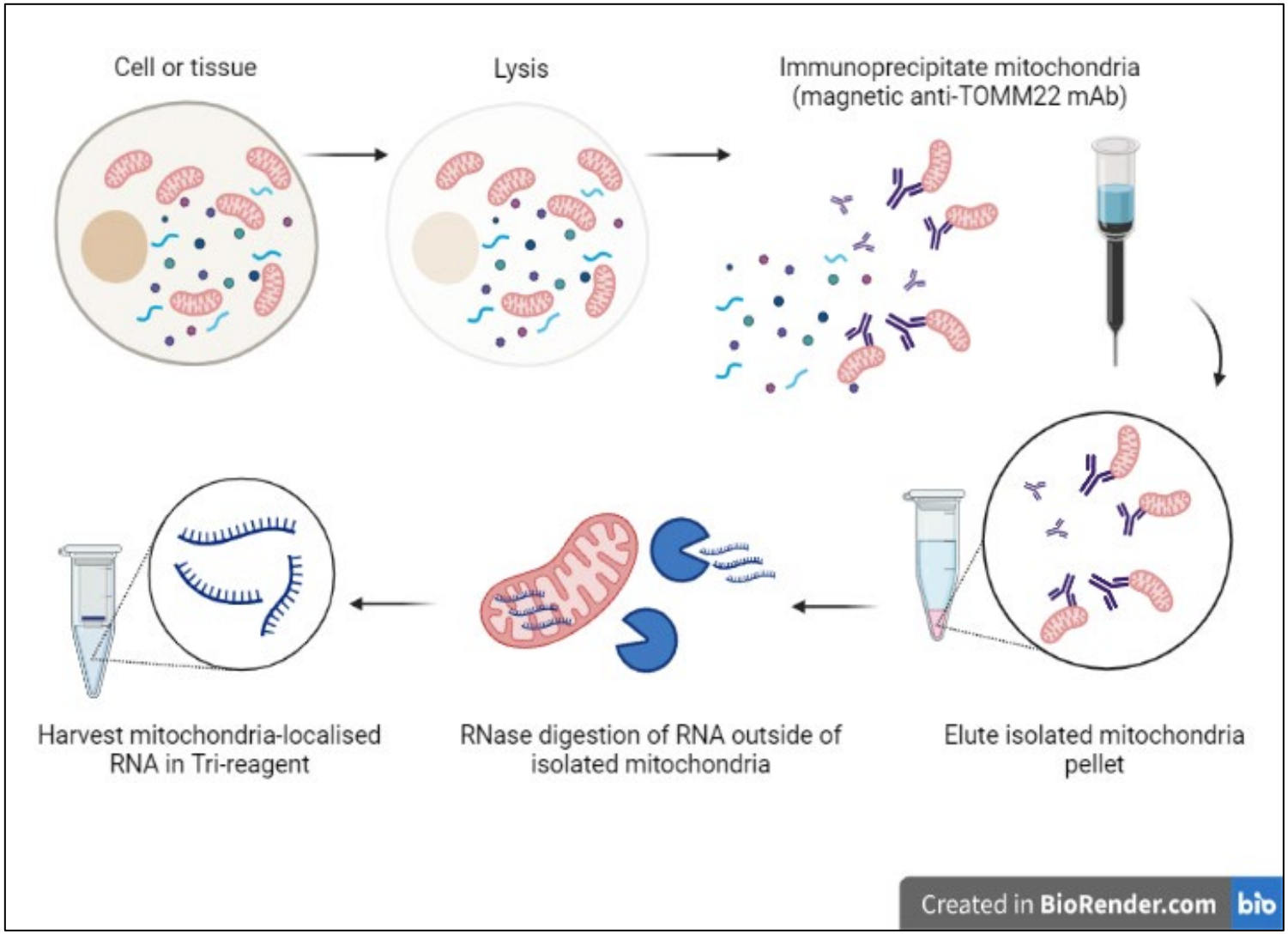
Cell or tissue
Lysis
Immunoprecipitate mitochondria
(magnetic anti-TOMM22 mAb)
Harvest mitochondria-localised
RNA in Tri-reagent
RNase digestion of RNA outside of
isolated mitochondria
Elute isolated mitochondria
pellet
Created in BioRender.com
bio

Figure 1.

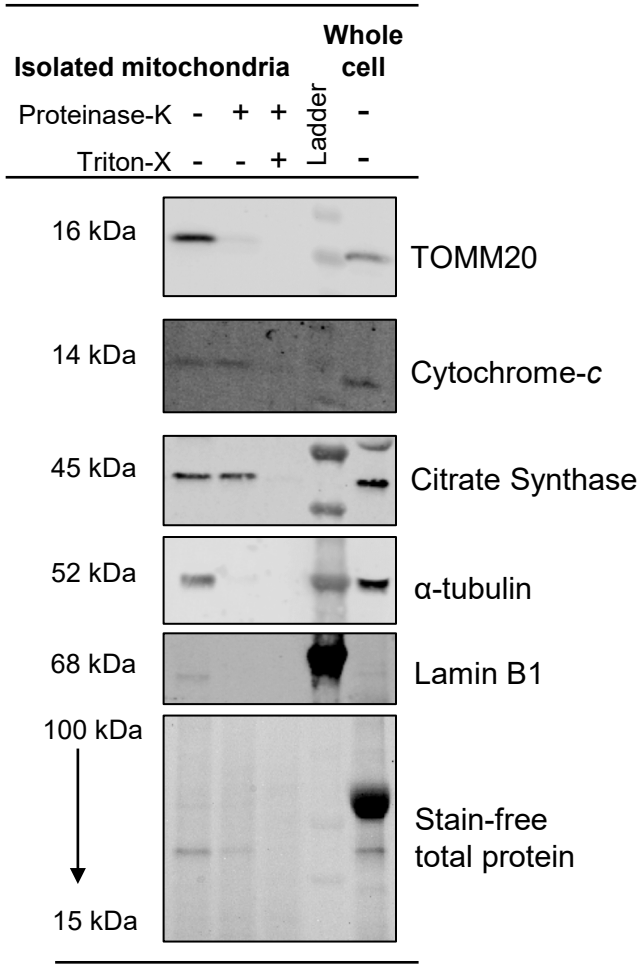
Isolated mitochondria
Whole cell
Proteinase-K - + + Ladder -
Triton-X - - + -
16 kDa
TOMM20
14 kDa
Cytochrome-c
45 kDa
Citrate Synthase
52 kDa
α-tubulin
68 kDa
Lamin B1
100 kDa
15 kDa
Stain-free
total protein

Figure 2.

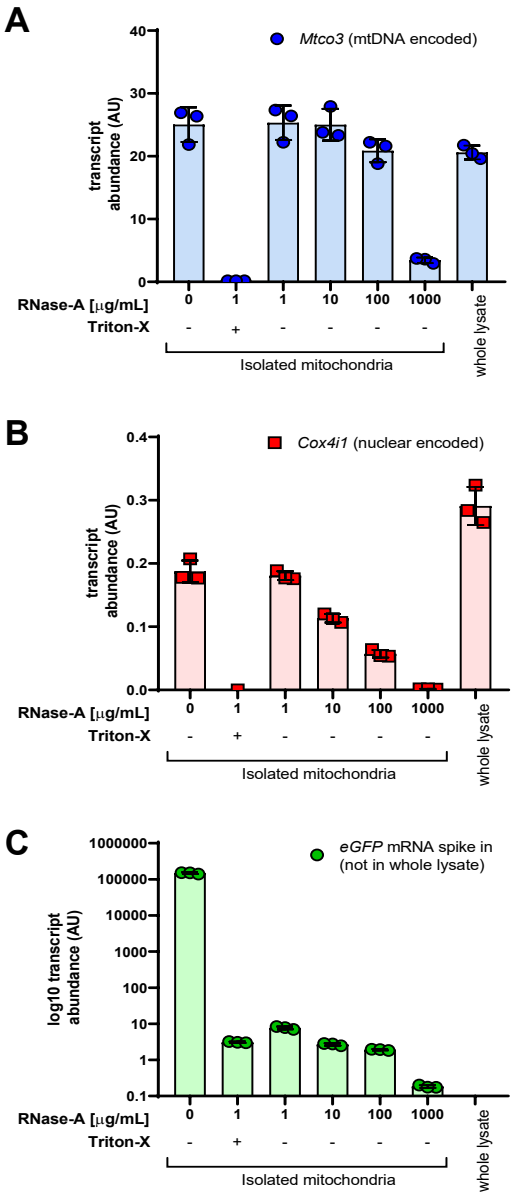
A
Mtco3 (mtDNA encoded)
transcript abundance (AU)
40
30
20
10
0
RNase-A [μg/mL]
0
1
1
10
100
1000
Triton-X
-
+
-
-
-
-
Isolated mitochondria
whole lysate
B
Cox4i1 (nuclear encoded)
transcript abundance (AU)
0.4
0.3
0.2
0.1
0.0
RNase-A [μg/mL]
0
1
1
10
100
1000
Triton-X
-
+
-
-
-
-
Isolated mitochondria
whole lysate
C
eGFP mRNA spike in (not in whole lysate)
log10 transcript abundance (AU)
1000000
100000
10000
1000
100
10
1
0.1
RNase-A [μg/mL]
0
1
1
10
100
1000
Triton-X
-
+
-
-
-
-
Isolated mitochondria
whole lysate

Figure 3.

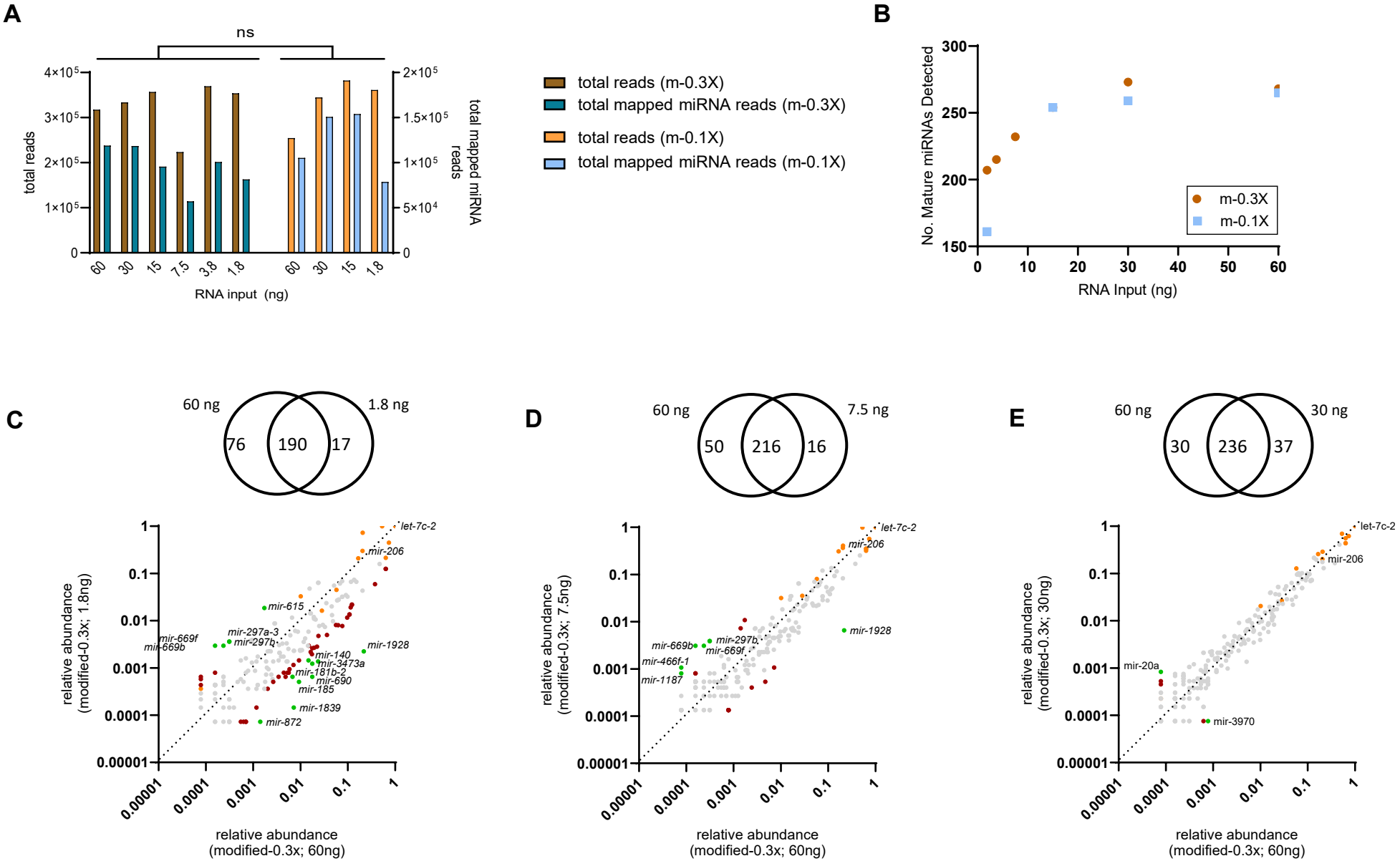
A
ns
total reads
total mapped miRNA reads
RNA input (ng)
total reads (m-0.3X)
total mapped miRNA reads (m-0.3X)
total reads (m-0.1X)
total mapped miRNA reads (m-0.1X)
B
No. Mature miRNAs Detected
RNA Input (ng)
m-0.3X
m-0.1X
C
60 ng
1.8 ng
76
190
17
relative abundance (modified-0.3x; 1.8ng)
relative abundance (modified-0.3x; 60ng)
let-7c-2
mir-206
mir-615
mir-669f
mir-669b
mir-297a-3
mir-297b
mir-1928
mir-140
mir-3473a
mir-181b-2
mir-690
mir-185
mir-1839
mir-872
D
60 ng
7.5 ng
50
216
16
relative abundance (modified-0.3x; 7.5ng)
relative abundance (modified-0.3x; 60ng)
let-7c-2
mir-206
mir-1928
mir-669b
mir-297b
mir-669f
mir-466f-1
mir-1187
E
60 ng
30 ng
30
236
37
relative abundance (modified-0.3x; 30ng)
relative abundance (modified-0.3x; 60ng)
let-7c-2
mir-206
mir-20a
mir-3970

Figure 4.

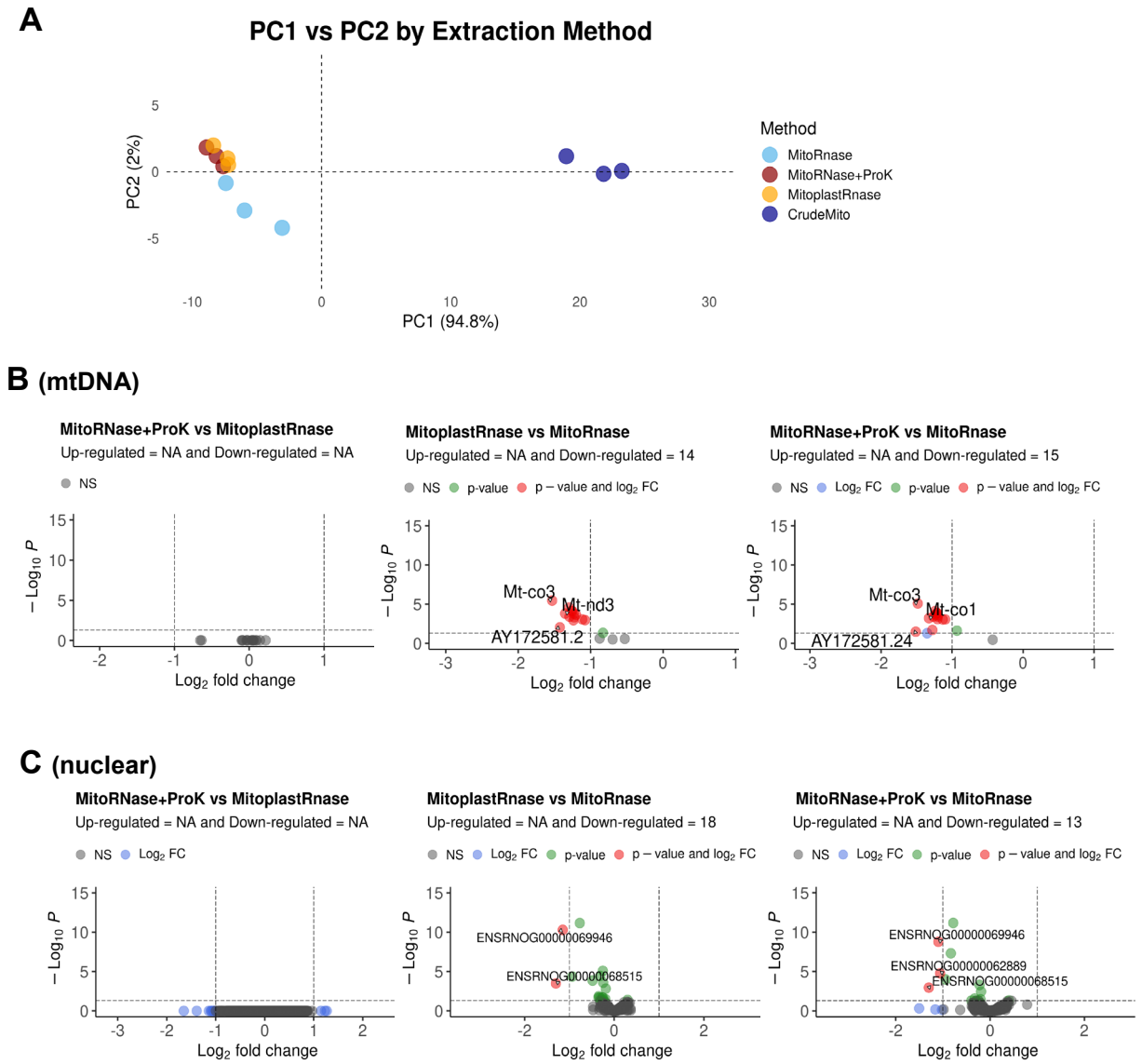
A
PC1 vs PC2 by Extraction Method
PC2 (2%)
PC1 (94.8%)
Method
MitoRnase
MitoRNase+ProK
MitoplastRnase
CrudeMito
B (mtDNA)
MitoRNase+ProK vs MitoplastRnase
Up-regulated = NA and Down-regulated = NA
NS
MitoplastRnase vs MitoRnase
Up-regulated = NA and Down-regulated = 14
NS p-value p – value and log2 FC
Mt-co3
Mt-nd3
AY172581.2
MitoRNase+ProK vs MitoRnase
Up-regulated = NA and Down-regulated = 15
NS Log2 FC p-value p – value and log2 FC
Mt-co3
Mt-co1
AY172581.24
– Log10 P
Log2 fold change
C (nuclear)
MitoRNase+ProK vs MitoplastRnase
Up-regulated = NA and Down-regulated = NA
NS Log2 FC
MitoplastRnase vs MitoRnase
Up-regulated = NA and Down-regulated = 18
NS Log2 FC p-value p – value and log2 FC
ENSRNOG00000069946
ENSRNOG00000068515
MitoRNase+ProK vs MitoRnase
Up-regulated = NA and Down-regulated = 13
NS Log2 FC p-value p – value and log2 FC
ENSRNOG00000069946
ENSRNOG00000062889
ENSRNOG00000068515

Figure 5.

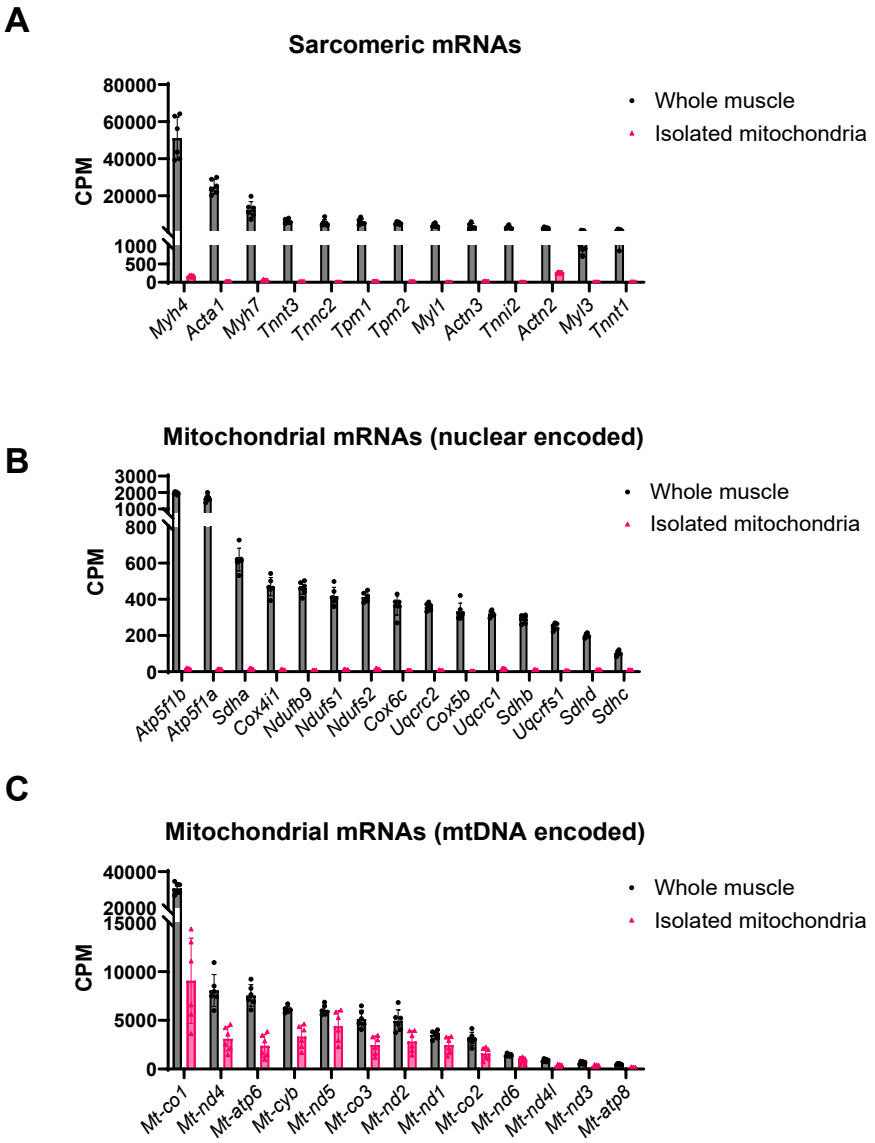
A
Sarcomeric mRNAs
CPM
80000
60000
40000
20000
1000
500
0
Whole muscle
Isolated mitochondria
Myh4
Acta1
Myh7
Tnnt3
Tnnc2
Tpm1
Tpm2
Myl1
Actn3
Tnni2
Actn2
Myl3
Tnnt1
B
Mitochondrial mRNAs (nuclear encoded)
CPM
3000
2000
1000
800
600
400
200
0
Whole muscle
Isolated mitochondria
Atp5f1b
Atp5f1a
Sdha
Cox4i1
Ndufb9
Ndufs1
Ndufs2
Cox6c
Uqcrc2
Cox5b
Uqcrc1
Sdhb
Uqcrfs1
Sdhd
Sdhc
C
Mitochondrial mRNAs (mtDNA encoded)
CPM
40000
20000
15000
10000
5000
0
Whole muscle
Isolated mitochondria
Mt-co1
Mt-nd4
Mt-atp6
Mt-cyb
Mt-nd5
Mt-co3
Mt-nd2
Mt-nd1
Mt-co2
Mt-nd6
Mt-nd4l
Mt-nd3
Mt-atp8

Figure 6.